Fermi-Surface Instability in the Heavy-Fermion Superconductor UTe_2

Q. Niu,[1] G. Knebel,[1] D. Braithwaite,[1] D. Aoki,[1,2] G. Lapertot,[1] G. Seyfarth,[3] J-P. Brison,[1] J. Flouquet,[1] and A. Pourret[1,*]

[1]*Université Grenoble Alpes, CEA, IRIG, PHELIQS, F-38000 Grenoble, France*
[2]*Institute for Materials Research, Tohoku University, Oarai, Ibaraki 311-1313, Japan*
[3]*Université Grenoble Alpes, EMFL, CNRS, Laboratoire National des Champs Magnétiques Intenses (LNCMI), 38042 Grenoble, France*

(Received 25 July 2019; revised manuscript received 30 October 2019; accepted 15 January 2020; published 26 February 2020)

Transport measurements are presented up to fields of 29 T in the recently discovered heavy-fermion superconductor UTe_2 with magnetic field H applied along the easy magnetization a axis of the body-centered orthorhombic structure. The thermoelectric power varies linearly with temperature above the superconducting transition, $T_{SC} = 1.5$ K, indicating that superconductivity develops in a Fermi liquid regime. As a function of field the thermoelectric power shows successive anomalies which appear at critical values of the magnetic polarization. Remarkably, the lowest magnetic field instability for $H \| a$ occurs for the same critical value of the magnetization (0.4 μ_B) than the first order metamagnetic transition at 35 T for field applied along the b axis. It can be clearly identified as a Lifshitz transition. The estimated number of charge carriers at low temperature reveals a metallic ground state distinct from LDA calculations indicating that strong electronic correlations are a major issue.

DOI: 10.1103/PhysRevLett.124.086601

Unconventional superconductivity (SC) in heavy-fermion systems is the consequence of the delicate interplay between competing magnetic and non-magnetic ground states. Recent studies on uranium based ferromagnetic superconductors have pointed out the interplay between magnetic fluctuations and a Fermi surface (FS) reconstruction on crossing the quantum phase transition at the ferromagnetic to paramagnetic instability [1]. The emergent picture is that the change of the amplitude of the ferromagnetic correlations and even the switch of the direction of the magnetic fluctuations are directly associated with a FS instability. A reinforcement of SC (RSC) has been observed in the three uranium based ferromagnetic superconductors URhGe [2], UCoGe [3], and UGe_2 [4]. In particular, in URhGe and UCoGe, RSC appears when a magnetic field is applied along the hard-magnetization b axis of this orthorombic crystal structure and it is linked to the increase of magnetic and electronic fluctuations due to the collapse of the Curie temperature in a field perpendicular to the easy magnetization axis. FS instabilities induced by a magnetic field, such as Lifshitz transitions (LTs) [5], have been observed in these heavy fermion materials [6–9] underlining the importance of the Zeeman splitting of the flat bands crossing the Fermi level. The respective role of such FS instabilities on the mechanism of RSC and the sole magnetic fluctuations is still an open question [6,10].

The recently discovered heavy-fermion superconductor UTe_2 [11,12] with superconducting transition temperature $T_{SC} = 1.6$ K, is one of the rare examples of heavy-fermion materials with $T_{SC} > 1$ K. In contrast to ferromagnetic UCoGe and URhGe, UTe_2 is a paramagnetic material but nevertheless it exhibits RSC [11,13,14] up to unrivalled magnetic field strengths among this class of materials. UTe_2 has an orthorhombic crystal structure. The easy magnetization axis is the a axis, and the c axis is the hard axis above 20 K [11]. For $H \| b$, there is a maximum of the magnetic susceptibility at $T_{\chi\,\max} \approx 35$ K, so that at $T = 2$ K the susceptibility is lowest for the b axis. This maximum of the susceptibility is related to the first order metamagnetic transition at $H_m = 35$ T [14–16] for the field applied along b axis at $T \to 0$ K. The superconducting upper critical field H_{c2} for $T \to 0$ K is very anisotropic: $H^a_{c2} = 6$ T, $H^c_{c2} = 12$ T, and $H^b_{c2} = H_m = 35$ T for a magnetic field applied along the a, c, and b axes, respectively. The values of H_{c2} for all directions highly exceed the Pauli limit. Spectacularly, for magnetic field applied along the b axis, $H_{c2}(T)$ is reinforced on approaching H_m [11,13].

The connection of a FS instability with the field-enhancement of SC has been most conclusively documented for URhGe [6,7]. In UCoGe, FS instabilities have been reported for field applied along the easy magnetiztion c axis. They have been identified as LTs linked to critical values of the magnetization [9]. However, RSC appears along the b axis in this system, possibly also linked to another FS instability [17]. The FS of UTe_2 has not been determined up to now. No quantum oscillations have been observed and recent photoemission spectroscopy experiments were not able to resolve the electronic band structure close to the Fermi level [18]. The first LDA band structure calculations obtained a Kondo semiconducting ground state

with very flat bands near the Fermi energy [12]. These results do not correspond to the real metallic electronic states observed at low temperature in UTe_2. By shifting the $5f$ level upward by 0.2 Ry in the LDA calculations, small FSs which occupy only 5% of the Brillouin zone appear [12], suggesting that UTe_2 would be a semimetallic system with heavy electronic states. In this Letter, we focus on the transport properties of UTe_2 under magnetic field applied along the easy magnetization a axis. In this direction, the magnetization above T_{SC} increases nonlinearly with the field, showing a tiny change of slope at 6.5 T, and starts to saturate above $H \approx 21$ T (reaching 1.05 μ_B at 40 T) [15]. We have observed in the different transport properties a series of anomalies as a function of magnetic field applied along the a axis. A LT near $H_1 = 5.6$ T occurs at the same value of magnetization, 0.4 μ_B, at which metamagnetism occurs for $H \| b$. Our experiments show that UTe_2 is a good metal with about one charge carrier per U atom which stresses the key role of electronic correlations.

Single crystals of UTe_2 were grown by chemical vapor transport with iodine as transport agent. The orientation of the crystals has been verified by Laue diffraction. In order to study the field dependence of the FS, we performed thermoelectric power (S), resistivity (ρ_{xx}), Hall effect (ρ_{xy}), and thermal conductivity (κ) measurements on different samples (labeled S1, S2, S3, S4) with residual resistivity ratios ($[\rho(300\ \mathrm{K})/\rho(1.6\ \mathrm{K})]$) of 30, 16, 38, and 15. S1, S2, and S3 have been prepared for experiments with heat or electric current along the a axis, while in S4 the current is applied along the c axis. S, κ, and ρ were measured with field along the a axis. ρ_{xy} was determined by applying the field along the b, c, and a axes in S2, S3, and S4, respectively. The temperature and field dependence of the different transport properties have been measured on sample S1 in CEA Grenoble down to 100 mK with a superconducting magnet up to 16 T and on samples S2 and S3 in a standard PPMS above 4K with field up to 9T. Furthermore, we performed measurements at LNCMI Grenoble using a ^{3}He cryostat up to 29 T on samples S1 and S4. S and κ have been measured using a standard "one heater–two thermometers" setup.

Figure 1 shows the magnetic field dependence of the different transport coefficients S, κ/T, R_{xx} and R_{xy} at 800 mK for $H \| a$. Different successive anomalies occur. For S1, H_{c2} defined by $S = 0$ corresponds to a sharp kink in κ/T. Above H_{c2}, $S(H)$ is negative and exhibits a peak at $H_1 = 5.6$ T, where $\kappa/T(H)$ also has a distinct change of slope. We note that a change in the field dependence of the magnetization appears at this field [15]. For S2, H_{c2} defined by $R = 0$ is slightly higher, but anomalies are observed in both R_{xx} and R_{xy} at H_1. For higher fields additional anomalies appear, most pronounced in $S(H)$ at $H_2 = 10.5$ T and $H_3 = 21$ T. The anomaly at H_2, corresponding to a broad minimum of R_{xx}, has been already identified previously [16]. Moreover, R_{xy} changes sign just

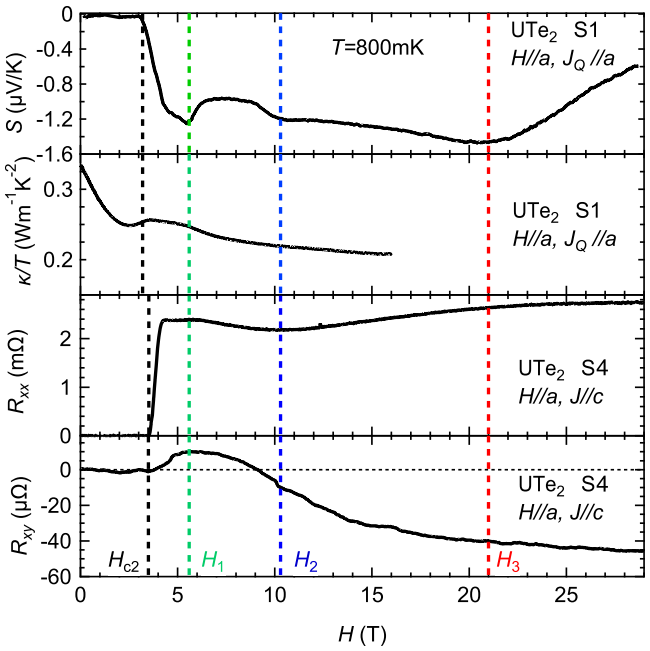

FIG. 1. Comparison of the magnetic field dependence of S, κ/T (S1), R_{xx} and R_{xy} (S4) at 800 mK in UTe_2. The different critical fields are represented by dashed vertical lines.

below H_2 related to a change of the dominant charge carriers. H_3 is only visible in S but appears to be linked to the entrance into the saturating regime of magnetization under field [15].

Figure 2 shows the field dependence of S up to 16 T [panel (a)] and up to 29 T [panel (b)] for different temperature ranges. Three anomalies can be observed above H_{c2} and followed as a function of temperature: the marked minimum at $H_1 = 5.6$ T is independent of temperature and merges with H_{c2} at a very low temperature. The anomalies at H_2 and H_3 have a strong temperature dependence. They can be followed up to 3 K, but get less pronounced. Above 3 K we observe a broad maximum around 4 T and a minimum around 12 T.

$H_{c2}(T)$ and the different anomalies H_1, H_2, and H_3 are displayed in the magnetic-field temperature phase diagram in Fig. 3. Using magnetization from Ref. [15], the corresponding magnetization scale, measured just above T_{SC}, is represented on the right axis. The key phenomenon is that FS changes are induced by crossing some critical values of magnetic polarization. We see that H_1 occurs when the magnetization reaches $M \approx 0.4\ \mu_B$/f.u. Remarkably, for $H \| b$ the magnetization is of the same order just below the magnetization jump at $H_m = 35$ T [15], which may indicate that the same band is affected in the two directions but the contribution of this band in the transport properties is much bigger for $H \| b$ [19,20]. At H_3, $M(H)$ starts to saturate.

The temperature dependence of S at $H = 0$ T is represented in Fig. 4(a). S is positive at high temperatures, and changes sign at 25 K, where the hard magnetization axis

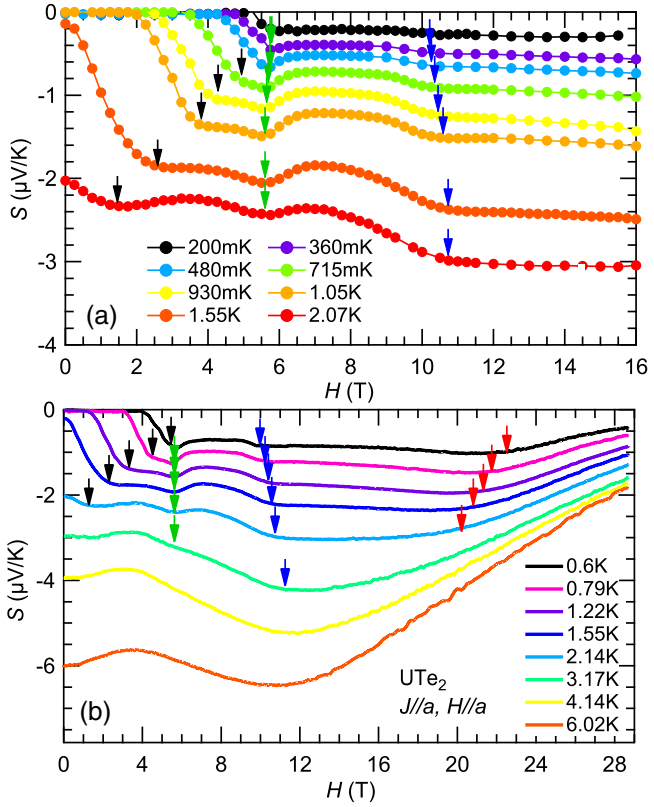

FIG. 2. Field dependence of S in UTe_2 (S1) for $H\|a$, (a) below 2 K up to 16 T measured using a superconducting magnet by averaging every point, and (b) below 6 K up to 29 T by sweeping continuously the magnetic field at LNCMI on sample S1. The arrows indicate the onset of the superconducting state and the position of the electronic instabilities.

changes from c to b axis and the longitudinal paramagnetic fluctuations start to develop along the a axis [21]. Decreasing temperature, S shows a broad minimum at around 12 K and goes linearly to zero below 10 K, as shown by the constant value of $S/T \approx -1\ \mu V/K^2$ (see inset of Fig. 4). A quasiconstant S/T strongly supports a Fermi liquid regime at low temperature in UTe_2 as already observed in resistivity measurements [11,12]. In contrast, this is not sufficient to explain the strong increase of the magnetization measured at low temperature for $H\|a$ [11,15]. Thus, the magnetic response dominated by the local U moments decouples from the quasiparticles at the Fermi level.

The field dependence of $S(T)$ is very weak, at least up to 9 T between 2 K and 70 K. S/T below 6 K is represented in Fig. 4(b). In zero field, S/T extrapolates to $-1\ \mu V/K^2$ at 0 K. For $H = H_1 = 5.6$ T, S/T shows a downward curvature exhibiting an approximate $T^{-\frac{1}{2}}$ dependence in S/T expected for a LT [22]. S/T can be fitted by the general T dependence near a neck disruption type LT, $S/T = a[0.75/T^* + 0.14(T^*T)^{-\frac{1}{2}}(1 - 0.29(Z/T))]$, represented by the black line. Here T^* is the characteristic size of the already existing FS nearby and Z characterizes the proximity of the system to the LT [22]. The fit gives $T^* \sim 20$ K, which corresponds to a Fermi pocket ~2 meV from the Fermi energy, and $Z = 0.37$ K represents 0.031 meV from the critical transition field [23]. For a LT, the main consequence on transport properties is not the change in

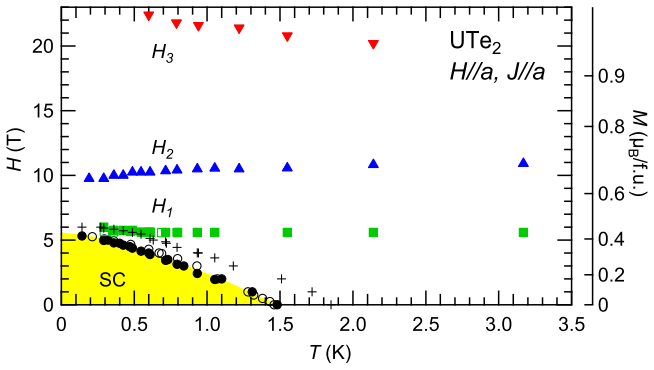

FIG. 3. Magnetic-field temperature phase diagram of UTe_2 (S1) for $H\|a$. H_{c2} determined by $S = 0$, the onset of the superconducting transition (crosses), and the different critical fields, H_1, H_2, and H_3, observed in S (full symbol), κ (open symbol), and ρ (crosses) are represented. These critical fields correspond to specific values of magnetization (right scale) measured at 1.4 K from Ref. [15].

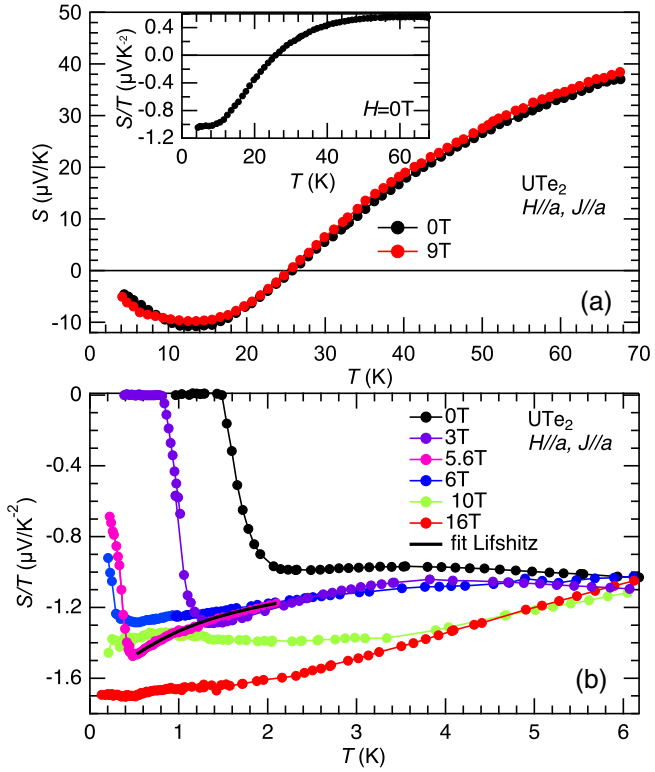

FIG. 4. (a) Temperature dependence of S at $H = 0$ and 9 T above 4 K (S2). The inset shows the temperature dependence of S/T for $H = 0$ T. (b) Temperature dependence of S/T for different magnetic field below 6 K (S1). S/T at 5.6 T is fitted using a temperature dependence expected for a LT.

the density of states but the change of the scattering rate [22,24]. Such a topological change of the FS will act as a trap for electrons in the scattering process from the main land FS (large k) to small pockets (small k) through impurities. So, the peak in S at H_1 is the finger print of a field-induced LT. For the anomalies occurring at H_2 and H_3 the analysis is less straightforward (they are broader and their field position slightly depends on temperature): no clear-cut signature of a LT is observed, leaving open the question regarding their microscopic nature.

In many heavy fermion systems field-induced LTs have now been identified [9,25–30] linked to critical values of the magnetization. The case of UTe_2 can be compared to the series of FS reconstructions observed in the ferromagnetic superconductor UCoGe when applying a field along the easy magnetization c axis, where up to five anomalies (H_1–H_5) have been detected. The Lifshitz character of the transitions in UCoGe has been confirmed by the direct observation of changes in the quantum oscillation frequencies [9]. Magnetization measurements for $H\|c$ do not show any detectable metamagnetic transition, especially not at the most marked anomaly at $H_4 \sim 16$ T, where the Hall effect changes sign from positive to negative. However, the anomaly at H_4 in UCoGe occurs by coincidence also for a magnetization of $M \approx 0.4\ \mu_B$/f.u. For the hard b axis in UCoGe, metamagnetism occurs at the same value of magnetization for $H \sim 45$ T [31]. In URhGe, magnetoresistivity experiments along the easy c axis suggest also a cascade of FS reconstructions at 4, 8, 11 T, but here already a large spontaneous FM moment ($m_0 \sim 0.4\ \mu_B$) characterizes the FM phase [32].

In many correlated metals, the absolute value of the dimensionless ratio $q = (SN_Ae/\gamma T)$ (γ is the Sommerfeld coefficient of the specific heat, e the elementary charge, and N_A the Avogadro number) is of the order of unity [33]. It has been argued that, in the zero-temperature limit, for scattering both in the Born and unitary limits, S/T becomes inversely proportional to the renormalized Fermi energy, and this leads to the observed correlation [34]. Let us recall that, when the carrier density is much lower than one itinerant electron per formula unit, a proportionally larger $|q|$ is expected. $S/T \approx -1\ \mu\mathrm{V/K^2}$ and $\gamma \approx 0.12$ J/(K^{2}mol) [12] yield $q \approx -0.8$, giving $n_U = (1/|q|) \approx 1.2$ carriers (electrons) per formula unit. This simple argument indicates that, as regards the value of S/T extrapolated at 0 K, the zero field ground state of UTe_2 is an heavy fermion metal with a significant number of charge carriers.

To further check the number of carriers in UTe_2, we have measured the Hall resistivity ρ_{xy} not only for $H\|a$ (see Fig. 1) but also for $H\|b$ and c axis. In Fig. 5, ρ_{xy}/H as a function of temperature measured at 9 T is represented for two magnetic field orientations, $H\|b$ and $H\|c$. For both field directions, ρ_{xy}/H shows a pronounced maximum around $T_{\chi\,\mathrm{max}} \approx 35$ K and changes sign below 5 K, see inset of Fig. 5. For $H\|c$, the Hall effect is much

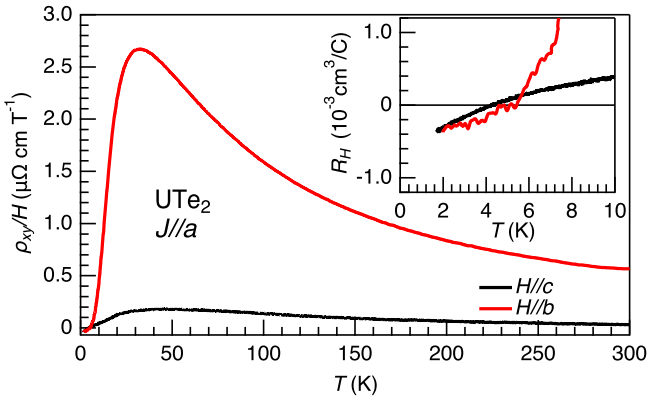

FIG. 5. ρ_{xy}/H as a function of temperature measured at 9 T for $H\|b$ (S2) and $H\|c$ (S3). The inset shows an enlargement of R_H in the low temperature region.

smaller, but the low temperature value at 2 K is similar, $\rho_{xy}/H \approx -36$ nΩ cm T^{-1}. The extrapolated value of the Hall coefficient at $T_{\mathrm{SC}} = 1.5$ K, $R_H = -3.8 \times 10^{-4}$ cm^3/C (corresponding to $\rho_{xy}/H = 39$ nΩ cm T^{-1}) where the influence of the skew scattering at $T_{\chi\,\mathrm{max}}$ can be neglected [35], gives a density of electrons $n = 1.6 \times 10^{22}$ cm^{-3}, taking a simple one band model. Using a volume per formula unit of $V_U = 88.9$ Å^3, this yields a number of carriers (electrons) per formula unit of $n_U = 1.4$. Another way to estimate the carrier number is to use thermodynamic data. Taking the average value of v_F, estimated from the slope of H_{c2} at T_{SC} [12], and $\gamma \approx 0.12$ J/(K^{2}mol) yields $n_U = 0.51$ carriers per uranium atom [36]. This value, which measures the density of the heaviest carriers (dominating γ and $(dH_{c2}/dT)|_{T_{\mathrm{SC}}}$), is slightly lower than the values estimated from the transport but still classifies UTe_2 as a good metal.

However, UTe_2 is a compensated metal, and we expect equal number of holes and electrons. Band structure calculations predict FSs from the hole and electron bands [12,18]. It has been recently observed that FS topology is very sensitive to the value of the Coulomb interaction [19] and also to the hypothesis of a rigid PM ground state [20]. Taking into account the two leg ladder type structure, rather large quasi-2D FSs, which are composed by heavier holes and lighter electrons cylinders, have been found with nesting properties quite similar to UGe_2 [20]. Recently, photoemission spectroscopy experiments have been reported [18]. Part of these experiments agree with the calculated band structure, however, the details of the band structure close to the Fermi level could not be resolved. The observation of an incoherent peak in the photoemission spectra has not been predicted. This confirms the importance of strong correlation effects.

In conclusion, our experiments establish a metallic and highly correlated ground state in UTe_2 distinct from a Kondo insulator ($\approx 1e^-/U$). A FS instability has been identified in different transport properties for field along the a axis. The temperature dependence of the anomaly in S at

H_1 confirms clearly the topological nature of this transition. The values of the critical polarization at which H_1 occurs for $H\|a$ and at which H_m occurs for $H\|b$ are remarkably similar indicating the strong interplay between magnetic polarization and electronic instabilities.

The authors thank K. Izawa, S. Hosoi, H. Harima, J. Ishizuka, Y. Yanase, and A. A. Varlamov for stimulating discussions. This work has been supported by the Université Grenoble Alpes and KAKENHI (Grants No. JP15H0082, No. JP15H0084, No. JP15K21732, No. JP19H00646, No. JP16H04006, and No. JP15H05745). We acknowledge support of the LNCMI-CNRS, member the European Magnetic Field Laboratory (EMFL).

*alexandre.pourret@cea.fr

[1] D. Aoki, K. Ishida, and J. Flouquet, J. Phys. Soc. Jpn. **88**, 022001 (2019).
[2] F. Lévy, I. Sheikin, B. Grenier, and A. D. Huxley, Science **309**, 1343 (2005).
[3] D. Aoki, T. D. Matsuda, V. Taufour, E. Hassinger, G. Knebel, and J. Flouquet, J. Phys. Soc. Jpn. **78**, 113709 (2009).
[4] I. Sheikin, A. Huxley, D. Braithwaite, J. P. Brison, S. Watanabe, K. Miyake, and J. Flouquet, Phys. Rev. B **64**, 220503(R) (2001).
[5] I. Lifshitz, Zh. Eksp. Teor. Fiz **38**, 1569 (1960) [Sov. Phys. JETP **11**, 1130 (1960)].
[6] E. A. Yelland, J. M. Barraclough, W. Wang, K. V. Kamenev, and A. D. Huxley, Nat. Phys. **7**, 890 (2011).
[7] A. Gourgout, A. Pourret, G. Knebel, D. Aoki, G. Seyfarth, and J. Flouquet, Phys. Rev. Lett. **117**, 046401 (2016).
[8] D. Aoki, G. Knebel, and J. Flouquet, J. Phys. Soc. Jpn. **83**, 094719 (2014).
[9] G. Bastien, A. Gourgout, D. Aoki, A. Pourret, I. Sheikin, G. Seyfarth, J. Flouquet, and G. Knebel, Phys. Rev. Lett. **117**, 206401 (2016).
[10] Y. Sherkunov, A. V. Chubukov, and J. J. Betouras, Phys. Rev. Lett. **121**, 097001 (2018).
[11] S. Ran, C. Eckberg, Q.-P. Ding, Y. Furukawa, T. Metz, S. R. Saha, I.-L. Liu, M. Zic, H. Kim, J. Paglione *et al.*, Science **365**, 684 (2019).
[12] D. Aoki, A. Nakamura, F. Honda, D. Li, Y. Homma, Y. Shimizu, Y. J. Sato, G. Knebel, J.-P. Brison, A. Pourret *et al.*, J. Phys. Soc. Jpn. **88**, 043702 (2019).
[13] G. Knebel, W. Knafo, A. Pourret, Q. Niu, M. Vališka, D. Braithwaite, G. Lapertot, M. Nardone, A. Zitouni, S. Mishra *et al.*, J. Phys. Soc. Jpn. **88**, 063707 (2019).
[14] S. Ran, I.-L. Liu, Y. S. Eo, D. J. Campbell, P. Neves, W. T. Fuhrman, S. R. Saha, C. Eckberg, H. Kim, J. Paglione, D. Graf, J. Singleton, and N. P. Butch, Nat. Phys. **15**, 1250 (2019).
[15] A. Miyake, Y. Shimizu, Y. J. Sato, D. Li, A. Nakamura, Y. Homma, F. Honda, J. Flouquet, M. Tokunaga, and D. Aoki, J. Phys. Soc. Jpn. **88**, 063706 (2019).
[16] W. Knafo, M. Vališka, D. Braithwaite, G. Lapertot, G. Knebel, A. Pourret, J.-P. Brison, J. Flouquet, and D. Aoki, J. Phys. Soc. Jpn. **88**, 063705 (2019).
[17] L. Malone, L. Howald, A. Pourret, D. Aoki, V. Taufour, G. Knebel, and J. Flouquet, Phys. Rev. B **85**, 024526 (2012).
[18] S.-i. Fujimori, I. Kawasaki, Y. Takeda, H. Yamagami, A. Nakamura, Y. Homma, and D. Aoki, J. Phys. Soc. Jpn. **88**, 103701 (2019).
[19] J. Ishizuka, S. Sumita, A. Daido, and Y. Yanase, Phys. Rev. Lett. **123**, 217001 (2019).
[20] Y. Xu, Y. Sheng, and Y. F. Yang, Phys. Rev. Lett. **123**, 217002 (2019).
[21] Y. Tokunaga, H. Sakai, S. Kambe, T. Hattori, N. Higa, G. Nakamine, S. Kitagawa, K. Ishida, A. Nakamura, Y. Shimizu, Y. Homma, D. Li, F. Honda, and D. Aoki, J. Phys. Soc. Jpn. **88**, 073701 (2019).
[22] A. A. Varlamov, V. S. Egorov, and A. V. Pantsulaya, Adv. Phys. **38**, 469 (1989).
[23] At finite temperature and/or in presence of impurities, the maximum of $|S/T|$ will be displaced near $Z = 0$.
[24] Y. M. Blanter, M. I. Kaganov, A. V. Pantsulaya, and A. A. Varlamov, Phys. Rep. **245**, 159 (1994).
[25] R. Daou, C. Bergemann, and S. R. Julian, Phys. Rev. Lett. **96**, 026401 (2006).
[26] A. Pourret, G. Knebel, T. D. Matsuda, G. Lapertot, and J. Flouquet, J. Phys. Soc. Jpn. **82**, 053704 (2013).
[27] A. Pourret, A. Palacio-Morales, S. Krämer, L. Malone, M. Nardone, D. Aoki, G. Knebel, and J. Flouquet, J. Phys. Soc. Jpn. **82**, 034706 (2013).
[28] H. Pfau, R. Daou, S. Lausberg, H. R. Naren, M. Brando, S. Friedemann, S. Wirth, T. Westerkamp, U. Stockert, P. Gegenwart, C. Krellner, C. Geibel, G. Zwicknagl, and F. Steglich, Phys. Rev. Lett. **110**, 256403 (2013).
[29] D. Aoki, G. Seyfarth, A. Pourret, A. Gourgout, A. McCollam, J. A. N. Bruin, Y. Krupko, and I. Sheikin, Phys. Rev. Lett. **116**, 037202 (2016).
[30] H. Pfau, R. Daou, S. Friedemann, S. Karbassi, S. Ghannadzadeh, R. Küchler, S. Hamann, A. Steppke, D. Sun, M. König, A. P. Mackenzie, K. Kliemt, C. Krellner, and M. Brando, Phys. Rev. Lett. **119**, 126402 (2017).
[31] W. Knafo, T. D. Matsuda, D. Aoki, F. Hardy, G. W. Scheerer, G. Ballon, M. Nardone, A. Zitouni, C. Meingast, and J. Flouquet, Phys. Rev. B **86**, 184416 (2012).
[32] G. Bastien, Ph.D. thesis, Université Grenoble Alpes, 2017.
[33] K. Behnia, D. Jaccard, and J. Flouquet, J. Phys. Condens. Matter **16**, 5187 (2004).
[34] K. Miyake and H. Kohno, J. Phys. Soc. Jpn. **74**, 1343 (2005).
[35] The Hall resistivity is linear with magnetic field up to 9 T, see Fig. S2 in Supplemental Material [36].
[36] See Supplemental Material at http://link.aps.org/supplemental/10.1103/PhysRevLett.124.086601 for more details about the carrier density estimation.